Magnetotransport properties of lithographically defined lateral Co/$Ni_{80}Fe_{20}$ wires

M. K. Husain and A. O. Adeyeye[a)]
Department of Electrical and Computer Engineering, Information Storage Materials Laboratory, National University of Singapore, 4 Engineering Drive 3, Singapore 117576

(Presented on 14 November 2002)

In this article we have investigated the magnetization reversal process of laterally defined coupled magnetic structures consisting of micron-sized sputtered Co and $Ni_{80}Fe_{20}$ wires lying side by side at temperatures ranging from 3 to 300 K. We have used a microfabrication technique to create an array of planar, laterally coupled magnetic wires made of two ferromagnetic materials. We observed two distinct peaks in the magnetoresistance (MR) curves corresponding to the magnetization reversals of Co and $Ni_{80}Fe_{20}$ wires. Below a critical temperature of 20 K we observed an asymmetric shift in the $Ni_{80}Fe_{20}$ peak position for both forward and reverse field sweeps due to the exchange coupling between the ferromagnetic ($Ni_{80}Fe_{20}$) and antiferromagnetic (Co–oxide at the interface of Co and $Ni_{80}Fe_{20}$ formed during fabrication) parts. The Co peaks gradually disappeared as the temperature was reduced. At low temperature we also observed that the $Ni_{80}Fe_{20}$ peaks in the MR loops are considerably shifted to larger fields corresponding to the increase in coercivity. © *2003 American Institute of Physics.* [DOI: 10.1063/1.1540179]

INTRODUCTION

Laterally defined micron and submicron ferromagnetic (FM) structures have received much attention because of the advances in lithographic and magnetic measurement techniques[1,2] as well as due to their potential for practical applications, for example, as data storage devices. Dramatic change in magnetic properties such as coercivity, saturation that occurs due to the change in lateral dimension provides the main motivation for studying these devices. It has been observed[2–6] that the magnetic properties are strongly dependent on the lateral size of FM due to the spatially varying demagnetizing field. With the recent development of magneto-electronic devices such as magnetic random access memory[7] and magnetoresistive head,[8] it is very important to understand the magnetization reversal mechanism of lithographically defined micron sized elements.

In the present work, we have studied the magnetization reversal of array of lithographically defined Co (40 nm)/$Ni_{80}Fe_{20}$(20 nm) micron sized wires at temperatures from 3 to 300 K. The fabricated structure is similar to the multilayer films, except that the wires are side-by-side as opposed to stacked film. The microfabricated planar structures are both magnetostatically and exchange coupled in contrast to the conventional multilayer magnetic thin films, where a spacer layer is used to exchange decouple the two consecutive layers. The fabrication of the planar structure is a parallel process when compared with the serial process of depositing thin multilayer films. The geometry is suitable with a slight modification for investigating a lateral magnetic tunneling junction.

We observed four distinct peaks in the magnetoresistance (MR) curves corresponding to the magnetization reversals of Co and $Ni_{80}Fe_{20}$ wires. With decreasing temperature the Co peaks gradually disappeared. As we cooled the sample we observed a noticeable increase in coercivity (H_C) and an asymmetric shift in the MR peak positions of the $Ni_{80}Fe_{20}$ wires below a critical point of 20 K. This asymmetric shift in the $Ni_{80}Fe_{20}$ peaks at low temperatures clearly indicates the exchange bias between the FM and antiferromagnetic (AFM) components. The latter appears due to the formation of Co–oxide at the edges of the Co wires during fabrication.

EXPERIMENTAL DETAILS

The magnetic structures were fabricated on a Si (001) substrate using the optical lithography and a combination of soft and hard lift-off techniques. Arrays of Si/Co (40 nm)/Al (100 nm) wires with width $w_1 = 6\ \mu$m and spacing $s = 4\ \mu$m were first fabricated using the standard optical lithography. Metallization was done by dc magnetron sputtering followed by lift-off in acetone. The working pressure and Ar gas flow rate during the film deposition were set at 10 mTorr and 10 standard cm^3/min (sccm), respectively, and a dc power of 100 W was used. The wires are 4 mm long and the array extends over a distance of 4 mm. In the next processing step, metallization of 20 nm thick $Ni_{80}Fe_{20}$ was carried out using dc sputtering. The final step of the fabrication process is the etching of the Al layer by a hard lift-off process in a weak solution of NaOH. By removing the Al layer we also removed $Ni_{80}Fe_{20}$ on top of Al. This wet etching process was carried out under an optical microscope and the removal of the Al layer was verified using a surface profiler. Complete removal of the $Ni_{80}Fe_{20}$ layer over the Co wires is

a)Author to whom correspondence should be addressed; electronic mail: eleaao@nus.edu.sg

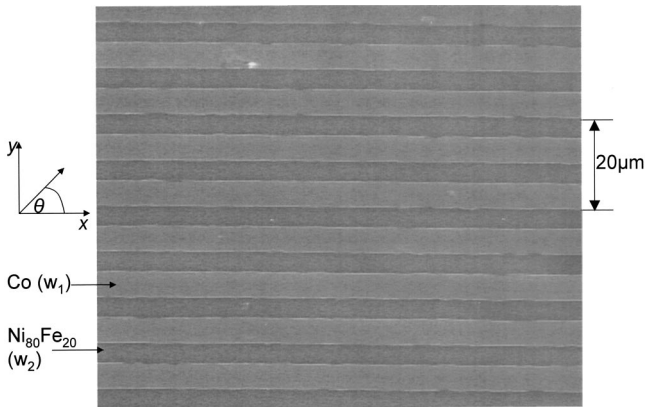

FIG. 1. Scanning electron micrograph of the lateral Co (40 nm)/$Ni_{80}Fe_{20}$ (20 nm) wire array.

confirmed by the color contrast of the two layers and from the surface profile. A scanning electron micrograph of the array of Co (40 nm)/$Ni_{80}Fe_{20}$ (20 nm) wires with $w_1 = 6\ \mu$m and $w_2 = 4\ \mu$m is shown in Fig. 1. Electrical contacts were made using a combination of standard optical lithography, metallization, and lift-off of 150 nm Al. The contacts were made parallel to the wire axis. For MR measurements, a dc sense current of 1 mA was passed through the current leads and the resistance was recorded automatically using a four terminal method as the in plane magnetic field was swept. The MR measurements were performed at temperatures ranging from 3 to 300 K. The low temperature measurements were performed using a Janis Model SVT Research Cryostat that enabled a temperature variation from 1.5 K to room temperature.

RESULTS AND DISCUSSION

Figure 2 shows the MR curves measured at 300 K for various field orientations. The MR responses are plotted as a percentage defined as

$$\mathrm{MR}\% = \frac{\mathrm{MR}(H) - \mathrm{MR}(H_{\mathrm{sat}})}{\mathrm{MR}(H_{\mathrm{sat}})} \times 100\%, \qquad (1)$$

where H_{sat} is the saturation field.

The intrinsic easy axis of the device is along the wires due to the shape anisotropy. Therefore the easy axis MR curves were measured in the field parallel to the wires ($\theta = 0°$). First a field of -1500 Oe was applied to saturate the magnetic wires in the negative x direction corresponding to point A in Fig. 2. As the magnetic field was increased at a constant rate, the MR curve was completely reversible until the field is of $\sim +24$ Oe (point B on the curve). At this field $Ni_{80}Fe_{20}$ wires switched in the positive x direction. At larger fields Co and $Ni_{80}Fe_{20}$ wires are magnetized antiparallel up to $H \sim +104$ Oe (point C on the curve), when the magnetization reversal of the Co wires occurs. As the field is swept to higher values, the magnetization of the entire array saturates along the positive x direction, corresponding to point D. The symmetrical $E-F-G-H$ curve was obtained after saturation in a large positive field and sweeping the field in the opposite direction. MR curves for fields applied at $\theta = 45°$ and 90° to the wires are shown in Fig. 2.

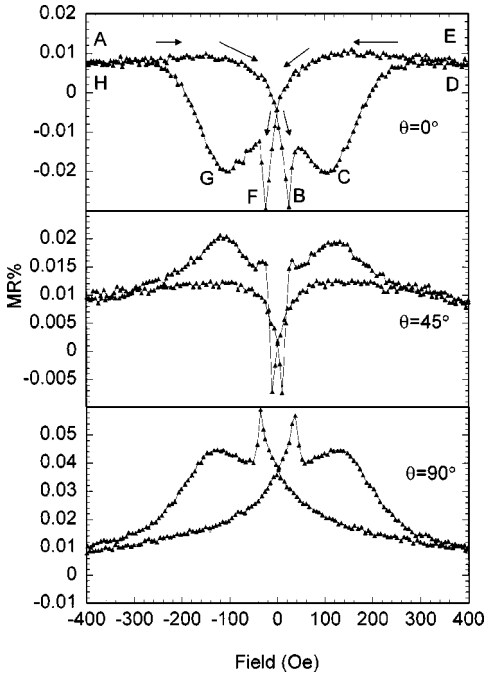

FIG. 2. MR curves of the lateral Co (40 nm)/$Ni_{80}Fe_{20}$ (20 nm) wire array at 300 K for various field orientations.

At $\theta = 45°$ we observe two symmetrical peaks on the MR curve corresponding to the switching field of $Ni_{80}Fe_{20}$. This may be due to the contribution of the components of the applied field along and across the wire axis.

For the field applied at $\theta = 90°$ we find that the MR peaks are inverted compared to the $\theta = 0°$ case. It is not surprising because the MR is dominated by the anisotropic magnetoresistance (AMR) which depends on the cosine of the angle between the current and the field direction. Sharp peaks on the MR curves corresponding to the switching of magnetization reveal the value of the coercive field.[2]

We have investigated the temperature dependence of the MR response of the fabricated structure. Figure 3 shows MR curves at various temperatures in the field perpendicular to the wires. Positions of the peaks shift noticeably with temperature. At low temperatures the Co peaks in Fig. 3 are smaller than those in Fig. 2. At further cooling the Co peaks (H_3 and H_4) gradually disappear. At 120 K the Co peaks are still detectable at a switching field of 388 Oe, whereas, at 7 K they completely disappear. The reason for this is still not understood.

For $T = 120$ K, the peak positions corresponding to the switching field of $Ni_{80}Fe_{20}$ wires are symmetrical. As the temperature is decreased we observed an unusual asymmetry in the peak positions for the forward and backward field sweeps. The $Ni_{80}Fe_{20}$ peaks (H_1, H_2) in the MR loops shift asymmetrically to higher fields. The asymmetric shift in the peak positions of MR loops at low temperatures indicates the appearance of the exchange bias (H_E) in the system. The biasing occurred due to the coupling of spins in the $Ni_{80}Fe_{20}$ (FM) and Co–oxide (AFM) when cooled below Néel tem-

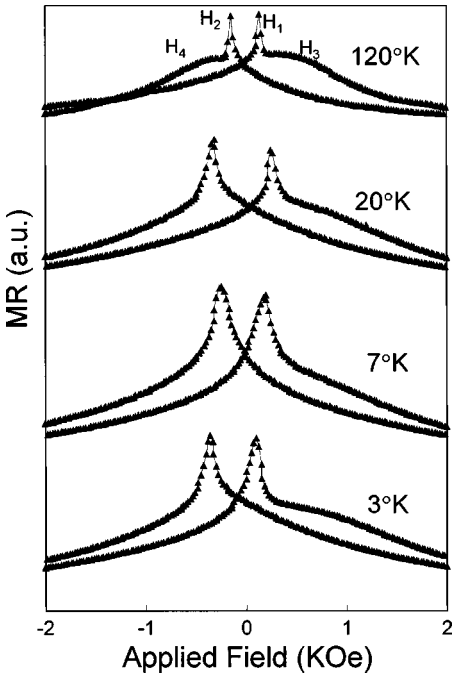

FIG. 3. MR curves of the lateral Co (40 nm)/$Ni_{80}Fe_{20}$ (20 nm) wire array for various temperatures with field applied along the *y* axis.

perature T_N. H_E depends strongly on the spin structure at the interface.[9–11]

The shift in peak positions is best described in terms of an effective internal "exchange field" H_E, defined as

$$H_E = 1/2|H_{c1} + H_{c2}|, \tag{2}$$

where H_{c1} and H_{c2} are the coercive fields corresponding to the right and left peaks of the MR loops.

Thus we are able to deduce the exchange field from the peak positions. The procedure we used to calculate H_E is in agreement with the method used by Spagna *et al.*[12] For example, when the temperature is 7 K an exchange bias field of 89 Oe is measured. This exchange bias can be attributed to the presence of Co–oxide at the interface of the wires. During fabrication, the Co wires were exposed to the atmosphere before the $Ni_{80}Fe_{20}$ film deposition. This resulted in natural oxidation of Co wire edges.

Shifting of the peaks to higher fields corresponds to the increase of the $Ni_{80}Fe_{20}$ coercivity with decreasing temperature. At $T = 20$ K, the coercivity H_C of $Ni_{80}Fe_{20}$ is 292 Oe. However as we cooled the sample to $T < 20$ K, the coercivity of the $Ni_{80}Fe_{20}$ wires decreased. For example, at 3 K we measured $H_C = 228$ Oe for the $Ni_{80}Fe_{20}$ wires. In order to further explore the low temperature dependence of H_C and H_E we have performed a systematic study of the asymmetric shift of the peaks as a function of temperature. Shown in Fig. 4 are the temperature dependences of H_C and H_E. For $T > 20$ K the exchange bias is absent and only ferromagnetic parts contribute to magnetization. As the temperature is reduced to 20 K a marked shift in the peak positions is observed for the $Ni_{80}Fe_{20}$ wires. From the asymmetric shift in the peak positions we were able to determine the exchange

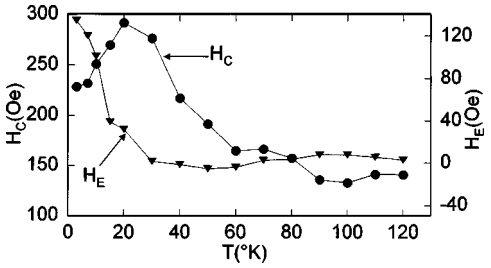

FIG. 4. Coercivity H_C and exchange bias H_E field vs temperature for a lateral Co (40 nm)/$Ni_{80}Fe_{20}$ (20 nm) wire array.

bias field of 35 Oe at 20 K. The blocking temperature T_B of the Co–oxide estimated from Fig. 4 is ~20 K. Possible antiferromagnetic components in our sample could be CoO and Co_3O_4. Bulk Co_3O_4 and CoO have T_N of about 30 K[13] and 290 K,[14,15] respectively. Therefore Co_3O_4 may be the main contributor to the AFM components. There might also be some contribution from other AFM phases.[11,16] When the spins in FM rotate they try to drag the AFM spins irreversibly increasing the coercivity. In Fig. 4 we observe a peak in H_C that is very close to T_B. This is in agreement with the experimental results obtained by others.[17–19] We observed that H_C decreases below 20 K. This may be due to the decoupling of the FM from AFM spins below T_B.

ACKNOWLEDGMENTS

This work was supported by the National University of Singapore (NUS) under Grant No. R263-000-180-112. M.K.H. would like to thank NUS for their Research Scholarship.

[1] A. Maeda, M. Kume, T. Ogura, K. Kuroki, T. Yamada, N. Nishikawa, and Y. Harada, J. Appl. Phys. **76**, 6667 (1994).
[2] A. O. Adeyeye, J. A. C. Bland, C. Daboo, and D. G. Hasko, Phys. Rev. B **56**, 3265 (1997); A. O. Adeyeye, G. Lauhoff, J. A. C. Bland, C. Daboo, D. G. Hasko, and H. Ahmed, Appl. Phys. Lett. **70**, 1046 (1997).
[3] K. Hong and N. Giordano, Phys. Rev. B **51**, 9855 (1955).
[4] W. Wernsdorfer, B. Doudin, D. Mailly, K. Hasselback, A. Beniot, J. Meier, J.-Ph Ansermet, and B. Barbara, Phys. Rev. Lett. **77**, 1873 (1996).
[5] J. Aumentado and V. Chandrasekhar, Appl. Phys. Lett. **74**, 1898 (1999).
[6] J. E. Wegrowe, D. Kelly, A. Franck, S. E. Gilbert, and J-Ph Ansermet, Phys. Rev. Lett. **82**, 3681 (1999).
[7] S. S. P. Parkin *et al.*, J. Appl. Phys. **85**, 5828 (1999).
[8] P. Ciureanu and S. Middelhoek, *Thin Film Resistive Sensors* (Institute of Physics, Bristol, 1992).
[9] M. Kiwi, J. Magn. Magn. Mater. **234**, 584 (2001).
[10] A. E. Berkowitz and K. Takano, J. Magn. Magn. Mater. **200**, 552 (1999).
[11] J. Nogués and I. K. Schuller, J. Magn. Magn. Mater. **192**, 203 (1999).
[12] S. Spagna, M. B. Maple, and R. E. Sager, J. Appl. Phys. **79**, 4926 (1996).
[13] W. Kundig, M. Kobelt, A. Appel, G. Constabaris, and R. H. Lindequist, J. Phys. Chem. Solids **30**, 819 (1969).
[14] M. D. Rechtin and B. L. Averbach, Phys. Rev. B **5**, 2693 (1972).
[15] L. Smardz, U. Köbler, and W. Zinn, J. Appl. Phys. **71**, 5199 (1992).
[16] M. Takahashi, A. Yanai, S. Taguchi, and T. Suzuki, Jpn. J. Appl. Phys. **19**, 1093 (1980).
[17] M. Tsunoda, Y. Tsuchiya, M. Konoto, and M. Takahashi, J. Magn. Magn. Mater. **171**, 19 (1997).
[18] R. P. Michel, A. Chaiken, Y. K. Kim, and L. E. Johnson, IEEE Trans. Magn. **32**, 4651 (1996).
[19] A. J. Devasahayam and M. H. Kryder, IEEE Trans. Magn. **32**, 4654 (1996).